Theano Papavassiliu, MD
Harald P. Kühl, MD
Meike Schröder, MD
Tim Süselbeck, MD
Olga Bondarenko, MD
Christoph K. Böhm, MD
Aernout Beek, MD
Mark M. B. Hofman, PhD
Albert C. van Rossum, MD, PhD

Published online before print
10.1148/radiol.2353040601
Radiology 2005; 236:57–64

Abbreviations:
ED = end diastole
EF = ejection fraction
ES = end systole
FISP = fast imaging with steady-state precession
LV = left ventricle
SD = standard deviation

[1] From Medical Clinic I (T.P., T.S.) and Dept of Radiology (M.S., C.K.B.), Univ Hosp of Mannheim, Theodor-Kutzer-Ufer 1-3, 68167 Mannheim, Germany; and Dept of Cardiology, VU Univ Medical Ctr, Amsterdam, the Netherlands (H.P.K., O.B., A.B., M.M.B.H., A.C.v.R.). Received Apr 8, 2004; revision requested Jun 18; revision received Jul 30; accepted Aug 25. T.P. supported by a grant from the Medical Faculty of the Univ of Mannheim. H.P.K. supported in part by grants from the Medical Faculty of the Rheinisch-Westfälische Technische Hochschule, Aachen, Germany, and the Grimmke-Stiftung, Düsseldorf, Germany. O.B. supported by grant 2001.158 from the Netherlands Heart Foundation. **Address correspondence to** T.P. (e-mail: *theano.papavassilliu@med.ma.uni-heidelberg.de*).

Authors stated no financial relationship to disclose.

Author contributions:
Guarantors of integrity of entire study, T.P., A.C.v.R.; study concepts, T.P., H.P.K., A.C.v.R., M.S.; study design, T.P., H.P.K., A.C.v.R., T.S., A.B., C.K.B.; literature research, T.P., O.B., T.S., C.K.B.; clinical studies, T.P., A.C.v.R.; data acquisition, T.P., H.P.K., A.C.v.R., M.M.B.H., O.B., A.B., M.S., C.K.B.; data analysis/interpretation, T.P., H.P.K., T.S.; statistical analysis, T.P., M.M.B.H., C.K.B., T.S.; manuscript preparation, T.P., H.P.K., A.C.v.R., M.S.; manuscript definition of intellectual content, A.B., M.M.B.H., T.S., C.K.B., O.B.; manuscript editing and final version approval, T.P., H.P.K., A.C.v.R.; manuscript revision/review, all authors

Effect of Endocardial Trabeculae on Left Ventricular Measurements and Measurement Reproducibility at Cardiovascular MR Imaging[1]

PURPOSE: To prospectively assess the effect of including or excluding endocardial trabeculae in left ventricular (LV) measurements and the reproducibility of these measurements at cine cardiovascular magnetic resonance (MR) imaging with true fast imaging with steady-state precession (FISP).

MATERIALS AND METHODS: The study was approved by the local ethics committee, and each subject gave informed consent before participating. Twenty healthy subjects and 20 consecutive patients underwent 1.5-T cardiovascular MR imaging. Seven to 12 short-axis views encompassing the entire LV were acquired by using true FISP. Endocardial and epicardial contours were traced manually. The data sets in each patient were analyzed twice: with inclusion of endocardial trabeculae in the LV cavity volume and with exclusion of endocardial trabeculae from the cavity volume. On the basis of these two contour sets, the end-diastolic (ED) and end-systolic (ES) LV volumes, ejection fraction (EF), and LV mass were calculated. Additionally, interobserver and interexamination reproducibility was assessed by using Bland-Altman analysis.

RESULTS: Compared with exclusion of trabeculae, inclusion of trabeculae in the LV cavity volume resulted in significantly larger ED and ES LV volumes (mean differences, 21 mL ± 11 [standard deviation] and 19 mL ± 33, respectively; $P < .001$) and lower EFs (mean difference, −2% ± 2; $P < .001$). The calculated LV mass was significantly smaller with inclusion than with exclusion of trabeculae (mean difference, −21 g ± 12; $P < .001$). All interobserver and interexamination limits of agreement based on inclusion of trabeculae, except those for EF measurements, were superior to those based on exclusion of trabeculae. At measurement reproducibility comparisons, differences in interobserver ED LV volume and LV mass and interexamination LV mass were statistically significant, favoring the inclusion of trabeculae in the LV cavity volume.

CONCLUSION: Trabeculae significantly affect quantifications of LV volume and mass. The superior reproducibility of LV measurements with the inclusion of endocardial trabeculae in the cavity volume favors this tracing algorithm for clinical use.

Left ventricular (LV) volumes and LV mass are powerful predictors of the prognosis associated with a variety of cardiovascular diseases (1–3). Therefore, the accurate measurement of these parameters is important for risk stratification and clinical management.

Cardiovascular magnetic resonance (MR) imaging performed by using conventional cine gradient-echo (ie, breath-hold segmented fast low-angle shot) sequences is an established reference standard for the assessment of LV volume and mass (4–6). Recent technical improvements have enabled the implementation of an alternative to the gradient-

echo cardiovascular MR imaging pulse sequence: true fast imaging with steady-state precession (FISP) (7). The true FISP sequence has become the technique of choice for assessing regional and global cardiac function because it yields substantially improved blood-tissue contrast and high temporal and spatial resolution (8,9). Use of this technique facilitates excellent endocardial border definition throughout the entire cardiac cycle and easier delineation of the borders, particularly in areas affected by slow blood flow, such as the regions around the papillary muscles and the LV trabeculae (10). Moreover, true FISP MR imaging allows visualization of even small endocardial trabeculae, which often could not be depicted by using conventional gradient-echo sequences owing to the lower blood-myocardium contrast and the lower spatial resolution.

The summation-of-sections method is the established reference standard for assessing LV volume and mass. At present, however, there is no clear consensus as to which tracing method for outlining the papillary muscles and the endocardial trabeculae should be used to achieve the most reliable and reproducible results. Thus, the aims of our study were to prospectively assess the effect of including or excluding endocardial trabeculae in LV measurements and to evaluate the reproducibility of these measurements at cine cardiovascular MR imaging performed with true FISP.

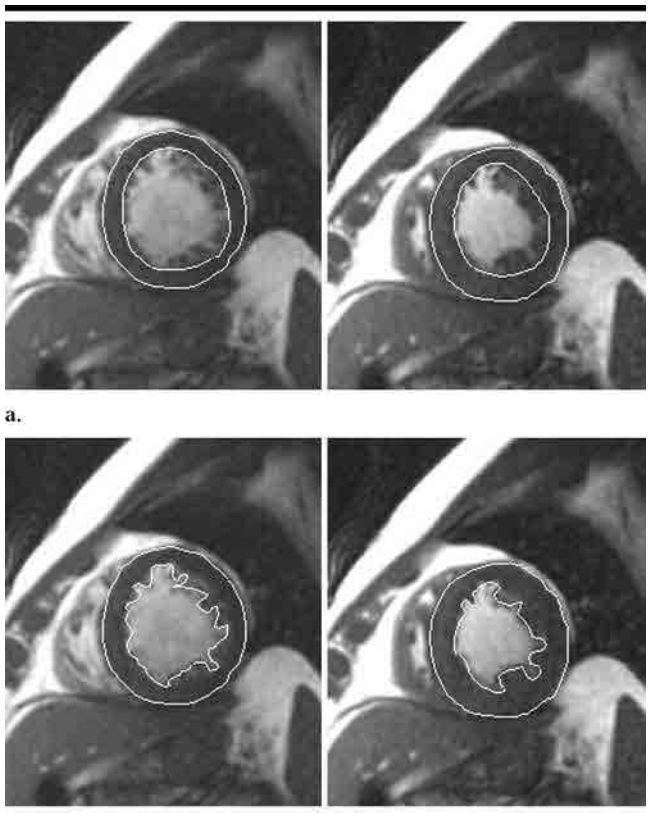

Figure 1. Single short-axis-view true FISP MR images (3.2/1.2) obtained in patient with impaired LV systolic function. **(a)** ED (left) and ES (right) images show inclusion of trabeculae in LV cavity volume. **(b)** ED (left) and ES (right) images show exclusion of trabeculae from LV cavity volume. The effect of trabeculae on the drawing of endocardial border contours is evident.

MATERIALS AND METHODS

Study Population

The study population consisted of 40 subjects (31 men, nine women). Twenty subjects (15 men, five women; mean age ± standard deviation [SD], 30 years ± 8; age range, 20–58 years) were healthy volunteers with no known risk factors for or history of cardiovascular disease, normal cardiac dimensions and geometry, and normal systolic function at echocardiography. The other 20 subjects (16 men, four women; mean age, 58 years ± 15; age range, 38–75 years) were consecutive patients with known histories of heart disease and impaired systolic function (mean ejection fraction [EF], 40% ± 16) who were examined from January to May 2003. All patients underwent electrocardiography, including levocardiography; echocardiography; and coronary angiography. Ten patients had dilated cardiomyopathy; six patients, ischemic cardiomyopathy; and four patients, hypertension-related heart disease. There was no statistically significant difference in sex between the volunteers and the patients, but there was a significant difference in age between the two groups. Each subject gave written informed consent before participating in the study, according to the requirements of the local ethics committee of VU University Medical Center, which approved our study.

Image Acquisition

All MR imaging examinations were performed by using a 1.5-T whole-body system (Magnetom Sonata; Siemens Medical Systems, Erlangen, Germany). A dedicated four-element, phased-array cardiac coil was used. The MR images were acquired during repeated end-expiratory breath holds. Scout MR images were obtained to plan the acquisition of the final double-oblique long- and short-axis views. Electrocardiographically gated cine MR images were then acquired by using a segmented steady-state precession sequence—true FISP—and the following parameters: 3.2/1.2 (repetition time msec/echo time msec), 35-msec temporal resolution, 1.4 × 1.8-mm in-plane spatial resolution, and 5-mm section thickness. Seven to 12 short-axis views that were 1 cm apart and encompassed the entire LV were acquired. The time required to obtain the short-axis sections ranged between 10 and 15 minutes.

Image Analysis and Determination of LV Parameters

The MR images were transferred to a separate workstation (Sun Sparcstation; Sun Microsystems, Mountain View, Calif). Image analysis was performed by using the MASS software package (Medis, Leiden, the Netherlands), as previously reported (11). The cine loops were reviewed, and the end-diastolic (ED) and end-systolic (ES) frames were identified for each short-axis section position. The ED frame was defined as the frame showing the largest cavity area, and

TABLE 1
LV Parameters Measured at MR Imaging

Parameter*	Outer Contours†	Inner Contours†	Absolute Difference†	Percentage Difference	Limits of Agreement	*P* Value
Healthy volunteers						
ED LV mass (g)	135 ± 32	149 ± 43	−14 ± 5	10	−24 to 4	<.001
EDV (mL)	154 ± 42	138 ± 33	16 ± 8	11	0 to 32	<.001
ESV (mL)	61 ± 16	53 ± 14	9 ± 5	15	−1 to 19	<.001
EF (%)	59 ± 4	61 ± 4	−2 ± 2	3	−6 to 2	<.05
Patients						
ED LV mass (g)	186 ± 50	214 ± 59	−28 ± 13	14	−54 to −2	<.001
EDV (mL)	234 ± 94	206 ± 88	27 ± 10	12	7 to 47	<.001
ESV (mL)	155 ± 98	133 ± 94	29 ± 45	20	−61 to 119	<.001
EF (%)	38 ± 16	40 ± 17	−2 ± 3	4	−8 to 4	<.05
All subjects						
ED LV mass (g)	160 ± 52	181 ± 61	−21 ± 12	12	−45 to 3	<.001
EDV (mL)	193 ± 81	171 ± 75	21 ± 11	12	−1 to 43	<.001
ESV (mL)	107 ± 84	91 ± 78	19 ± 33	19	−47 to 85	<.001
EF (%)	49 ± 16	51 ± 17	−2 ± 2	4	−6 to 2	<.001

Note.—Measurements of LV parameters included the trabeculae (outer contours) and excluded the trabeculae (inner contours) from the cavity volume.
* EDV = ED LV volume, ESV = ES LV volume.
† Data are mean values ± SDs.

TABLE 2
Interobserver Reproducibility of Measurements in 40 Subjects

	Outer Contours			Inner Contours			
Measurement*	Mean ± SD	Limits of Agreement	RC	Mean ± SD	Limits of Agreement	RC	*P* Value
EDV (mL)	−3.7 ± 5.4	−14.3 to 7.0	14	0.4 ± 10.1	−19.0 to 20.0	20	.05
ESV (mL)	−4.8 ± 6.8	−18.0 to 8.5	16	−1.5 ± 8.5	−18.0 to 15.0	17	.36
EF (%)	1.2 ± 2.8	−4.4 to 6.8	6	−0.7 ± 2.4	−5.3 to 4.0	5	.11
LV mass (g)	3.8 ± 6.0	−7.8 to 15.5	14	1.7 ± 9.0	−16.0 to 19.5	18	.03

Note.—RC = repeatability coefficient.
* EDV = ED LV volume, ESV = ES LV volume.

the ES frame was defined as the frame showing the smallest cavity area. The most basal section was the section that at ED and ES still showed a wall thickness that was compatible with the LV myocardium and that extended over at least 50% of the myocardial circumference. At ES, this most basal section could also show a part of the LV outflow tract or the mitral valve leaflets. The most basal section could differ by one section position between ED and ES.

In each patient, the first observer (T.P., with 4 years experience in cardiac MR imaging) determined the ED and ES frames, as well as the number and end-section position of short-axis sections used for the analysis, according to the described criteria. This information was subsequently used by the second observer (M.S., with 3 years experience in cardiac MR imaging).

Epicardial and endocardial contours were outlined manually on each ED and ES short-axis-view MR image. For each patient and image section, the contrast and brightness settings were optimized to achieve the best possible contrast between the myocardium and the LV cavity. The papillary muscles were outlined separately and included in the myocardial mass. The papillary muscles were identified on the long- and short-axis MR images, and their location and extent were correlated with each other. On the basal sections, the papillary muscles were usually disconnected from the LV wall and could be easily identified. On the more apical sections, where the papillary muscles were attached to the wall, it was sometimes difficult to clearly differentiate these muscles from the trabeculae. When the papillary muscles could not be clearly distinguished from the trabeculae, they were treated as trabeculae.

Right ventricular trabeculations arising from the interventricular septum and the epicardial fat were excluded from the LV mass. So that the effect of trabeculae on LV parameter measurements could be specifically assessed and the variability associated with manual tracing of the epicardial borders and the papillary muscles could be minimized, we changed neither the boundaries of the epicardium nor the contours of the papillary muscles during the tracing of the endocardium with either method (with trabeculae included and with trabeculae excluded). However, to minimize observer bias, there was a time interval of at least 1 week between the two tracing convention–based analyses of each data set. Thus, only the contours of the epicardial boundaries and of the papillary muscles were stored. The following tracing conventions were used:

Inclusion of trabeculae in LV cavity volume.—Trabeculum was defined as a structure 1.5 mm or larger in diameter that was protruding into the LV cavity and was attached to the LV wall. During tracing of the endocardial borders, in a separate window there was always a continuous movie display of the section being evaluated so that the trabeculae could be visually followed during contraction and relaxation. This display enabled better differentiation of the LV trabeculae from

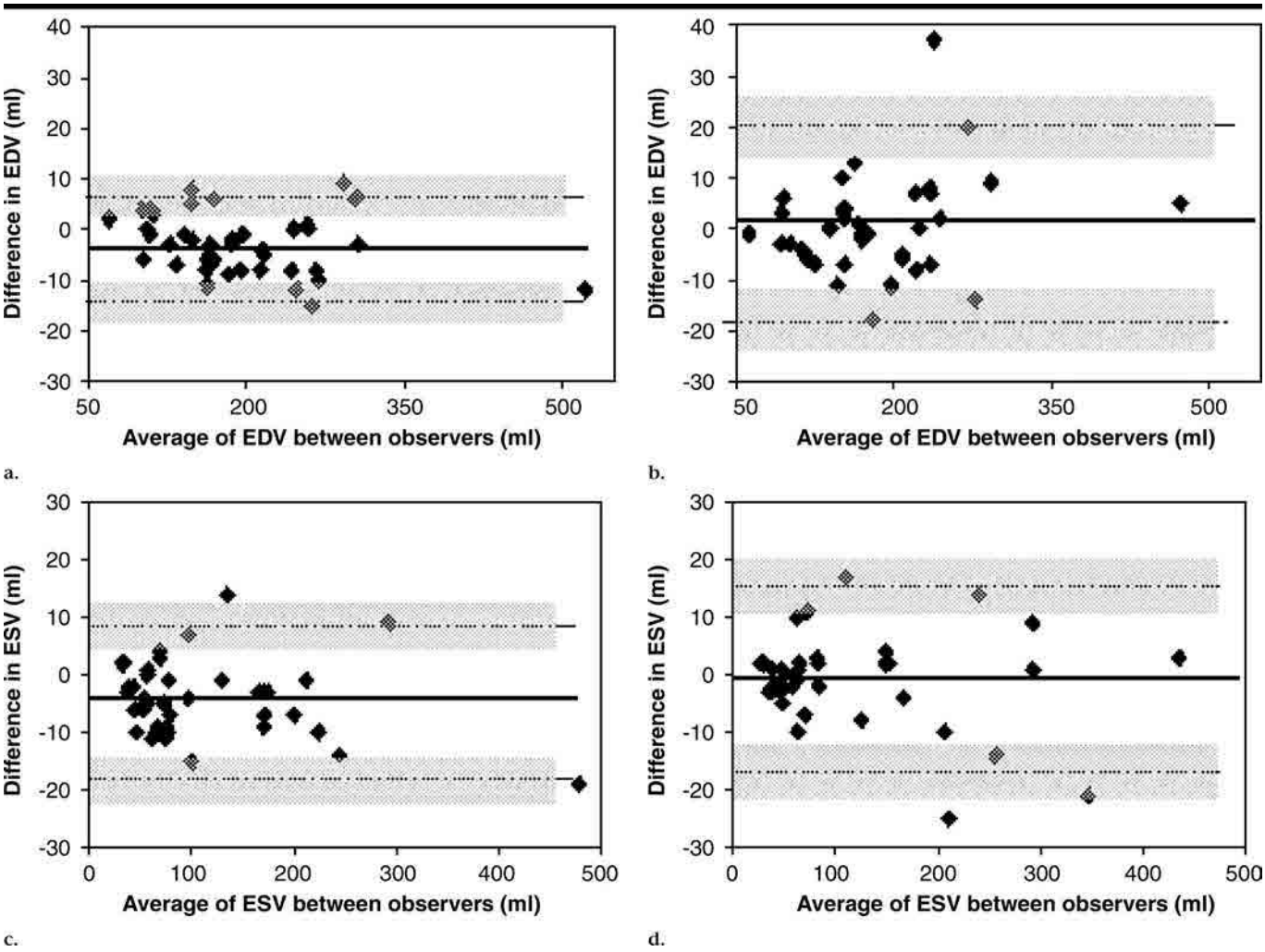

Figure 2. Bland-Altman plots depict interobserver agreement regarding LV measurements obtained when trabeculae were included in (**a**, **c**, **e**, and **g**) or excluded from (**b**, **d**, **f**, and **h**) the LV cavity volume. On each plot, solid line represents mean value of the differences in measurements between the two observers, dotted lines represent ±2 SDs, and shaded areas represent confidence intervals. The mean value of the two measurements is plotted along the x-axis, and the difference (observer 1 measurement minus observer 2 measurement) is plotted along the y-axis. EDV = ED LV volume, ESV = ES LV volume *(Fig 2 continues).*

the LV wall, particularly on the ES frames. During endocardial tracing, trabeculae were included in the LV cavity volume. This inclusion resulted in a smooth endocardial contour that was almost parallel to the epicardial contour. An example of tracing performed by using this inclusion (outer-contour) convention is depicted in Figure 1a.

Exclusion of trabeculae from LV cavity volume.—With use of the exclusion (inner-contour) tracing method, trabeculae were excluded from the LV cavity volume. The same definition of *trabeculum* was applied, and a movie display was available. Structures smaller than 1.5 mm in diameter, structures not clearly attached to the myocardial wall, and structures with a faint appearance on the cardiovascular MR images were not considered to be trabeculae. The resulting endocardial contour had an irregular, serrated shape and was clearly distinct from the smooth epicardial contour. An example of tracing performed by using the inner-contour convention is depicted in Figure 1b.

On the basis of these two contour sets, the ED and ES LV volumes, EF, and LV mass at ED were calculated. ED and ES LV volumes were calculated by using a modification of the Simpson rule. The EF was calculated as follows: EF = [(EDV − ESV)/EDV] · 100%, where EDV is the ED LV volume and ESV is the ES LV volume. The LV mass (M_{LV}) was calculated from the diastolic phase as follows: $M_{LV} = 1.05 \cdot (V_{epi} - V_{endo})$, where V_{epi} is the epicardial volume and V_{endo} is the endocardial volume. The average image analysis time was 40 minutes per subject (ie, per group of subject images).

To assess interobserver measurement reproducibility, a second independent and blinded observer (M.S.) repeated the LV measurements in each data set by using the same two tracing conventions. This observer was blinded to the subject details (ie, patient names, ages, and medical histories) and to the first observer's findings. For assessment of interexamination measurement variability, six subjects returned for repeat MR imaging at least 1 week after the first examination.

Statistical Analyses

Data are presented as means ± SDs. The two tracing algorithms were compared in terms of LV volume and mass

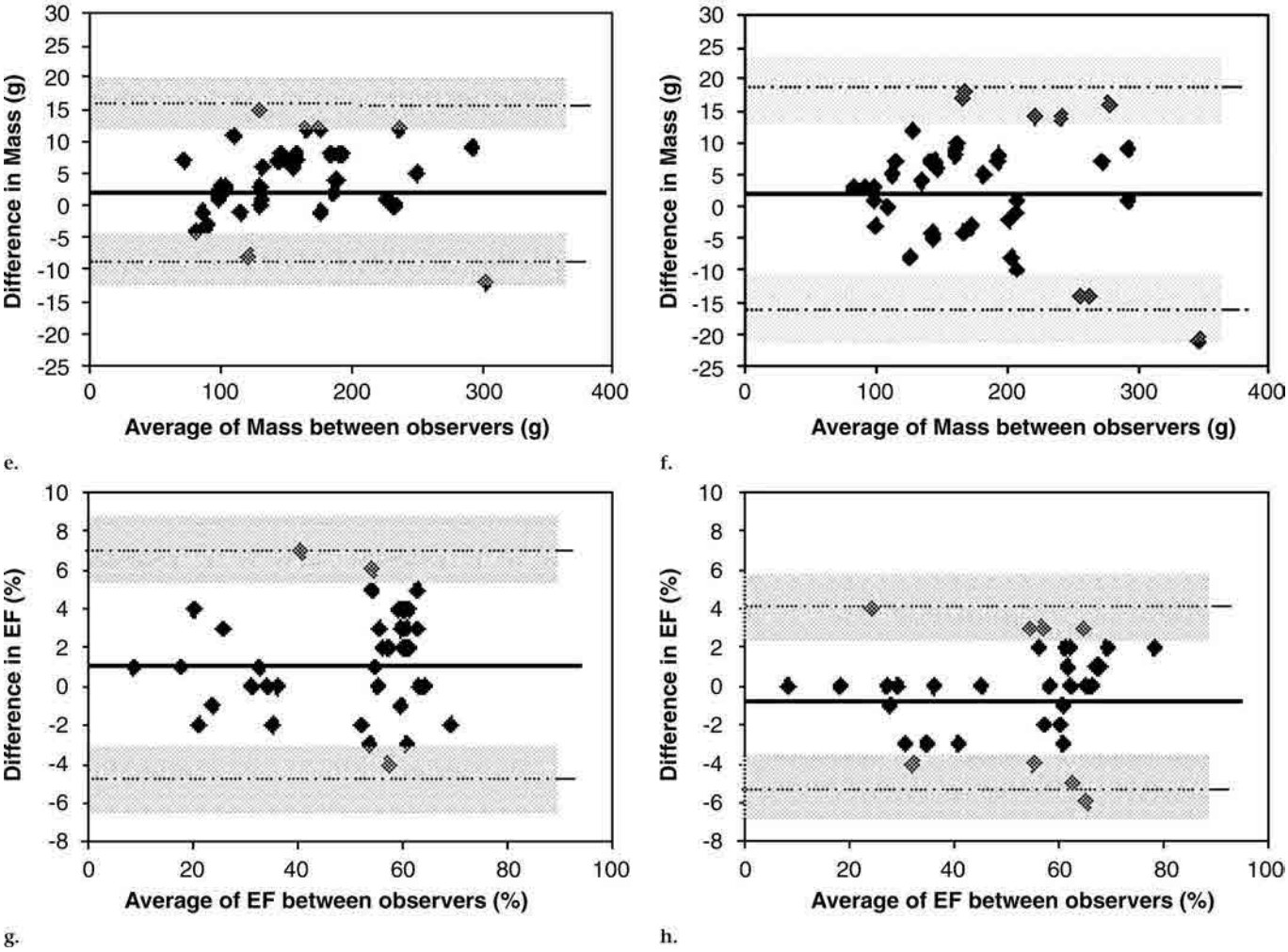

Figure 2 *(continued)*. Agreement between the two independent observers was better when measurements were obtained with the trabeculae included in the cavity volume (**a**, **c**, **e**, and **g**) than when measurements were obtained with the trabeculae excluded from the cavity volume (**b**, **d**, **f**, and **h**).

measurements by using the paired *t* test. Agreement between the two tracing algorithms was assessed by using the method described by Bland and Altman (12). Interobserver measurement reproducibility also was assessed by using Bland-Altman analysis, which yielded the mean difference, the limits of agreement of the mean difference (difference ± 1.96 SDs), and the corresponding 95% confidence intervals. Moreover, the coefficients of repeatability for each tracing algorithm and for the preceding parameters (ED volume, ES volume, EF, and LV mass) were assessed, with the coefficient of repeatability calculated as two times the SDs of the differences between the two measurements. Similarly, interexamination measurement reproducibility was assessed by using Bland-Altman analysis. In addition, the coefficient of variability (equal to the SD of the difference between the two measurements divided by the mean of the two measurements, expressed as a percentage) was calculated.

The statistical significance of differences in interobserver and interexamination reproducibility was assessed by using an extension of the Bland-Altman method. A log transformation of the squared differences between the two measurements was performed. If the squared difference was zero, it was replaced by half of the next smallest value. A two-tailed paired *t* test of the logged squared differences for the two tracing algorithms (12,13) could then be performed. At all comparisons, $P < .05$ was considered to indicate a significant difference.

Power calculations to assess the sample sizes needed in this study could not be performed in advance because no estimate of the SD of the difference between the outer- and inner-contour tracing algorithms was available. However, after acquiring data from our first 10 subjects, we did perform a power calculation (two-sided paired *t* test performed with SAS, version 8.2 software [SAS Institute, Cary, NC]) on the basis of the SD estimated from these data. According to this calculation, the number of subjects needed to establish a power of 90% (with $\alpha = .05$) was 12 for the comparison between the outer- and inner-contour tracing conventions performed by one observer. The sample sizes needed to establish a power of 90% for the assessment of interobserver agreement on measurements obtained by using outer-contour tracing (ie, ED and ES LV volumes, LV mass, and EF) and a power of 80% for the assessment of interobserver agreement on measurements obtained by using inner-contour

TABLE 3
Interexamination Reproducibility of Measurements in Six Subjects

	Outer Contours			Inner Contours			
Measurement*	Mean ± SD	Limits of Agreement	CV (%)	Mean ± SD	Limits of Agreement	CV (%)	*P* Value
EDV (mL)	4.17 ± 5.70	−7.0 to 15.3	3	0.33 ± 14.70	−28.0 to 29.0	9	.06
ESV (mL)	−1.00 ± 6.00	−12.7 to 10.7	8	−6.00 ± 8.00	−21.7 to 9.7	11	.36
EF (%)	0 ± 2.00	−3.9 to 3.9	3	2.00 ± 2.00	−1.9 to 5.9	3	.13
LV mass (g)	1.17 ± 5.50	−9.6 to 11.9	4	4.700 ± 7.00	−9.0 to 18.0	5	.046

Note.—CV = coefficient of variability.
* EDV = ED LV volume, ESV = ES LV volume.

tracing were 13 and 40 subjects at maximum, respectively.

RESULTS

The inclusion of trabeculae in the LV cavity volume (outer-contour method), as compared with the exclusion of trabeculae (inner-contour method), resulted in significantly larger ED and ES LV volumes and significantly smaller EF and LV mass values in all subjects (Table 1).

Analysis of the agreement between measurements obtained by the two independent observers (with each tracing algorithm) was performed (Table 2). The limits of agreement and corresponding 95% confidence intervals for measurements obtained with the inclusion of trabeculae in the LV cavity volume—with the exception of those for EF measurements—were narrower than those for measurements obtained with the exclusion of endocardial trabeculae (Fig 2). In addition, coefficients of repeatability—with the exception of those for EF calculations—were lower, indicating better reproducibility, when measurements that included trabeculae in the LV cavity volume were assessed. Differences in the interobserver reproducibility of LV mass and ED LV volume measurements were statistically significant, favoring the outer-contour convention (Table 2).

Analysis of agreement between the measurements at two MR imaging examinations obtained by using the two tracing methods was performed (Table 3). The limits of agreement for measurements obtained with the inclusion of trabeculae in the cavity volume—with the exception of those for EF measurements—were narrower than those for measurements obtained with the exclusion of endocardial trabeculae. In addition, coefficients of variability—with the exception of those for EF calculations—were better when measurements that included trabeculae in the cavity volume were assessed. Differences in the interexamination reproducibility of LV mass measurements were statistically significant, favoring the inclusion of trabeculae (Table 3).

DISCUSSION

A substantial portion of the myocardial mass consists of trabecular tissue (14). This tissue is not appreciated with most of the in vivo cardiac imaging methods used to evaluate cardiac function. Cardiovascular MR imaging performed by using conventional cine gradient-echo sequences is the current standard of reference for assessing ventricular function. However, true FISP cine cardiovascular MR imaging, being independent of inflow enhancement, has been proved to yield superior contrast between the myocardium and blood (15) and excellent image quality, and, thus, to enable detailed visualization of even small endocardial trabeculae. The effect of endocardial trabeculae on the measurement of LV parameters due to this excellent contrast between the ventricular cavity and the surrounding myocardium is not fully known. Thus, in this study we focused on the endocardial trabeculae, their influence on LV measurements, and the reproducibility of these measurements with use of true FISP cine MR imaging.

The study results demonstrate that in patients and healthy subjects, LV trabeculae significantly affect all LV measurements. Compared with the inclusion of trabeculae in the LV cavity volume, the exclusion of endocardial trabeculae resulted in systematically smaller LV volumes and larger EF and LV mass values.

There currently is no clear consensus as to which method of tracing the papillary muscles and endocardial trabeculae should be used to achieve the most reliable and reproducible results. Several investigators have reported normal cardiovascular MR imaging indexes of LV volume and mass that were obtained by using different tracing conventions. To our knowledge, Lorenz et al (16) reported the first normal ranges for LV mass and volume that were obtained by using a conventional free-breathing gradient-echo sequence. Because of signal intensity averaging, a clear delineation of the endocardial trabeculae was not possible with use of this technique. In another study involving the use of a gradient-echo sequence with breath holding, Marcus et al (11) reported normal LV volume and mass values. There was a difference in the ED LV mass values obtained in the Lorenz et al and Marcus et al studies, however. This difference may have been partially related to differences in data acquisition technique (breath holding vs no breath holding) and study subject age range between the two studies. A third main difference between the two studies was related to the drawn contour of the endocardial border: Marcus et al (11) drew a larger contour around the endocardial border, which resulted in lower LV mass values compared with those in the Lorenz et al (16) study.

A study by Moon et al (13), in which FISP and fast low-angle shot MR image acquisitions were compared for the assessment of LV volume, mass, and function, revealed small but significant differences in ED and ES LV volumes and LV mass between the two techniques. There were two reasons for these differences: The endocardial contour was drawn larger and the epicardial contour was drawn smaller on the FISP MR images. On fast low-angle shot MR images, the papillary muscles can appear larger and confluent with the myocardium. Moreover, blood between the trabeculations depicted on fast low-angle shot images can appear to be a part of the myocardium and thereby result in lower LV volumes and higher LV mass values compared with the values calculated by using FISP images. These differences in mea-

surements between conventional gradient-echo and steady-state precession pulse sequences were also confirmed in the recently published study of Alfakih et al (17).

The importance of including or excluding the endocardial trabeculae and the papillary muscles in LV measurements obtained with conventional gradient-echo pulse sequences was previously emphasized by Ibrahim et al (18) and Marcus et al (19). Ibrahim et al used cine breath-hold gradient-echo cardiovascular MR imaging to measure the LV volumes, EF, and LV mass in 52 healthy subjects and found that the inclusion of the papillary muscles in the blood pool, as compared with the exclusion of the papillary muscles and the trabeculae, resulted in systematically higher ED and ES LV volumes and lower LV mass values ($P < .001$). The exclusion of trabeculae from the blood pool resulted in the highest EF values ($P < .001$). The findings in our study are consistent with these results.

Marcus et al (19) measured the LV mass in 40 healthy subjects and quantified the portion of the mass that was contributed by the most basal section and by the endocardial trabeculae. The results indicated that the mean contribution to the ED LV mass from the papillary muscles was 6 g ± 5, or 4% ± 3. It was most striking that the ES LV mass was larger than the ED LV mass by a mean of 5 g ± 9, or 3% ± 6, when the most basal section and the papillary muscles were included in the LV mass measurements. Marcus et al hypothesized that the endocardial trabeculae were responsible for the apparent increase in mass during systole.

The endocardial border is not a sharply demarcated line between blood and myocardium; rather, it is a trabecular zone with a complex border. This factor leads to clinically relevant differences between measurements obtained by using different tracing conventions, as described earlier. Thus, comparing published LV measurement results is very difficult. Additionally, published normal ranges of cardiovascular MR imaging–based LV mass and volume values cannot be easily adopted because different tracing conventions were used. These differences emphasize the need for uniform criteria for outlining the endocardial contour. Functional true FISP cardiac MR imaging, as compared with conventional gradient-echo MR imaging, yields a high level of endocardial detail and allows easier discrimination of the endocardial borders. Therefore, true FISP cardiovascular MR imaging may become the technique of choice for assessing LV volume and mass.

The clinical value of a specific analysis method is determined on the basis of not only the accuracy but also the reproducibility of the method. Therefore, we sought to determine whether one of the two described tracing conventions was superior to the other in terms of measurement reproducibility. The interobserver and interexamination reproducibility of LV volume and mass measurements obtained by including endocardial trabeculae in the LV cavity volume was superior to that of measurements obtained by excluding endocardial trabeculae. There are two main reasons for these differences: *(a)* Because of their small size, trabeculae are difficult to differentiate from the LV wall, and, thus, tracing is complicated. *(b)* The decision of which endocardial trabeculae to exclude from the cavity volume is very challenging and varies considerably, even when experienced observers perform the tracing.

On the basis of our observations, we suggest that endocardial trabeculae be excluded from the myocardial mass and included in the LV cavity volume. This tracing convention may be easier to follow for different observers and thus result in less observer variability. Thus, the superior interobserver and interexamination reproducibility of measurements obtained by including endocardial trabeculae in the LV cavity volume favors this tracing algorithm for clinical use.

Another advantage of including trabeculae in the LV cavity volume is that measurements of regional wall thickness and systolic wall thickening can be expected to be more realistic. Peters et al (20) found that measurements of myocardial wall strain derived from tagged MR images showed correlation between regions of the trabeculae and the papillary muscles and regions of high strain, and this correlation led to an overestimation of the function in the lateral wall.

There were limitations to our study. First, during systole, the trabeculae and the papillary muscles are less well defined owing to compression and folding. In the current study, the compressed trabeculae appeared as a segment of continuous myocardial tissue in some regions at ES, and this made accurate delineation of the endocardial borders very challenging. Therefore, a movie display of the section being evaluated was always available. This display allowed us to differentiate the trabeculae from the LV wall at ES by integrating the visual information obtained continuously during the cardiac cycle. Nevertheless, identifying the trabecular tissue at ES remained difficult in some cases, which might support the use of the convention with which endocardial trabeculae are excluded from the LV cavity volume. In these cases, the inner-contour convention allowed easier delineation of the endocardial border. This finding explains the similar coefficients of reproducibility for measurements of the ES LV volume and the EF.

Second, the best tracing algorithm is probably that which is the most accurate and the most reproducible. Because we measured LV parameters in vivo, we were not able to test for accuracy. Therefore, we sought to assess whether one of the two described tracing conventions was superior to the other in terms of reproducibility. Third, the sample size of examined subjects in our study was relatively small; however, the sample represented a population with a wide spectrum of cardiac disorders.

In conclusion, endocardial trabeculae significantly affect the quantification of LV volume and mass. The superior reproducibility of LV measurements obtained by including endocardial trabeculae in the cavity volume favors this tracing algorithm for clinical use. Our findings may aid in reaching a consensus on uniform tracing criteria to standardize cardiovascular MR imaging measurements of LV parameters.

References

1. Levy D, Garrison RJ, Savage DD, Kannel WB, Castelli WP. Prognostic implications of echocardiographically determined left ventricular mass in the Framingham Heart Study. N Engl J Med 1990; 322:1561–1566.
2. Koren MJ, Devereux RB, Casale PN, Savage DD, Laragh JH. Relation of left ventricular mass and geometry to morbidity and mortality in uncomplicated essential hypertension. Ann Intern Med 1991; 114:345–352.
3. Casale PN, Devereux RB, Milner M, et al. Value of echocardiographic measurement of left ventricular mass in predicting cardiovascular morbid events in hypertensive men. Ann Intern Med 1986; 105:173–178.
4. Semelka RC, Tomei E, Wagner S, et al. Normal left ventricular dimensions and function: interstudy reproducibility of measurements with cine MR imaging. Radiology 1990; 174:763–768.
5. Semelka RC, Tomei E, Wagner S, et al. Interstudy reproducibility of dimensional and functional measurement between cine magnetic resonance imaging studies in the morphologically abnormal left ventricle. Am Heart J 1990; 119:1367–1373.
6. Pattynama PM, Lamb HJ, Van der Velde EA, et al. Left ventricular measurements with cine and spin echo MR imaging: a study of reproducibility with variance component analysis. Radiology 1993; 187: 261–268.

7. Oppelt A, Graumann R, Barfuss H. FISP: a new fast MRI sequence. Electromedica 1986; 54:15–18.
8. Plein S, Bloomer TN, Ridgway JP, Jones TR, Bainbridge GJ, Sivananthan MU. Steady-state free precession magnetic resonance imaging of the heart: comparison with segmented k-space gradient-echo imaging. J Magn Reson Imaging 2001; 14:230–236.
9. Barkhausen J, Ruehm SG, Goyen M, Buck T, Laub G, Debatin JF. MR evaluation of ventricular function: true fast imaging with steady-state precession versus fast low-angle shot cine MR imaging—feasibility study. Radiology 2001; 219:264–269.
10. Thiele H, Nagel E, Paetsch I, et al. Functional cardiac MR imaging with steady-state free precession (SSFP) significantly improves endocardial border delineation without contrast agents. J Magn Reson Imaging 2001; 14:362–363.
11. Marcus JT, DeWaal LK, Gotte MJ, van der Geest RJ, Heethaar RM, Van Rossum AC. MRI-derived left ventricular function parameters and mass in healthy young adults: relation with gender and body size. Int J Card Imaging 1999; 15:411–419.
12. Bland JM, Altman DG. Statistical methods for assessing agreement between two methods of clinical measurement. Lancet 1986; 1:307–310.
13. Moon JC, Lorenz CH, Francis JM, Smith GC, Pennell DJ. Breath-hold FLASH and FISP cardiovascular MR imaging: left ventricular volume differences and reproducibility. Radiology 2002; 223:789–797.
14. Anderson RH, Becker AE. The ventricles II: the morphologically left ventricle—the interventricular septum. In: Anderson RH, Becker AE, eds. Cardiac anatomy. London, England: Gower Medical Publishing, 1980; 10–20.
15. Fang W, Peerless FS, Bundy J, et al. Evaluating left ventricular function using real-time trueFISP: a comparison with conventional MR techniques (abstr). In: Proceedings of the Eighth Meeting of the International Society for Magnetic Resonance in Medicine. Berkeley, Calif: International Society for Magnetic Resonance in Medicine, 2000; 308.
16. Lorenz CH, Walker ES, Morgan VL, Klein SS, Graham TP Jr. Normal human right and left ventricular mass, systolic function, and gender differences by cine magnetic resonance imaging. J Cardiovasc Magn Reson 1999; 1:7–21.
17. Alfakih K, Plein S, Thiele H, Jones T, Ridgway JP, Sivananthan MU. Normal human left and right ventricular dimensions for MRI as assessed by turbo gradient echo and steady-state free precession imaging sequences. J Magn Reson Imaging 2003; 17:323–329.
18. Ibrahim T, Weniger M, Schwaiger M. Effect of papillary muscles and trabeculae on left ventricular parameters in cine magnetic resonance images (abstr). J Cardiovasc Magn Reson 1999; 1:319.
19. Marcus JT, Kuijer JPA, Götte RM, et al. Left ventricular mass measured by magnetic resonance imaging: effect of endocardial trabeculae on the observed wall thickness (abstr). J Cardiovasc Magn Reson 2000; 2:301–302.
20. Peters DC, Ennis DB, McVeigh ER. High-resolution MRI of cardiac function with projection reconstruction and steady-state free precession. Magn Reson Med 2002; 48:82–88.